Measurements of electron avalanche formation time in W-band microwave air breakdown

Alan M. Cook,[a] Jason S. Hummelt, Michael A. Shapiro, and Richard J. Temkin
Plasma Science & Fusion Center, Massachusetts Institute of Technology, 167 Albany St., Cambridge, Massachusetts 02139, USA

(Received 1 June 2011; accepted 29 July 2011; published online 23 August 2011)

We present measurements of formation times of electron avalanche ionization discharges induced by a focused 110 GHz millimeter-wave beam in atmospheric air. Discharges take place in a free volume of gas, with no nearby surfaces or objects. When the incident field amplitude is near the breakdown threshold for pulsed conditions, measured formation times are ~0.1–2 μs over the pressure range 5–700 Torr. Combined with electric field breakdown threshold measurements, the formation time data shows the agreement of 110 GHz air breakdown with the similarity laws of gas discharges.
 [doi:10.1063/1.3626383]

Electron avalanche ionization discharge (breakdown) induced in gas by a microwave electric field is an important phenomenon in the use of high-power microwaves (HPM). For applications that use the breakdown plasma to manipulate a microwave beam, the time required for the breakdown to occur is a critical parameter. The time delay between the application of the microwave field and the appearance of a high-density discharge plasma is a sum of two components: the time spent waiting for an initial free electron to appear in the gas to seed the avalanche (statistical delay) and the formation time of the avalanche.[1,2] Technology that relies on prompt breakdown in the presence of high-power microwaves, such as receiver-protector switches, typically make use of a seed electron source to eliminate the statistical delay. In that case, the growth time of a discharge plasma in response to an incident HPM pulse is limited by the avalanche formation time, which is typically on the order of tens of nanoseconds to one microsecond. Recent research has studied the roles of statistical and formative delay in HPM breakdown, including modeling seed electron sources[3–5] and measuring the effect of external ultraviolet radiation on breakdown delay time.[6]

With the continued development of megawatt-level millimeter-wave sources,[7–9] it has become possible to study discharges in a free volume of gas at frequencies between the microwave and optical regimes. Data in this regime aid in the design of high-power millimeter-wave technology.[10,11] Recent studies of millimeter-wave breakdown have observed formation of periodic arrays of plasma filaments that propagate toward the radiation source.[12–15] Detailed numerical models are able to reproduce many of the surprising features of the pattern formation and propagation seen in these experiments.[16–19]

In this paper, we study breakdown in air induced by a focused 110 GHz millimeter-wave beam, over the pressure range 5–700 Torr. There are no surfaces near the breakdown region to emit electrons, so the observed breakdown phenomena are governed completely by properties of the bulk gas. While the breakdown plasma forms a filament pattern at high pressure as seen in the experiments of Hidaka *et al.*,[14] here we study the formation of the initial electron avalanche during the rise of the microwave pulse, before the first filament forms. We record cumulative breakdown probability distributions with 30–60 time measurements at each pressure and use them to deduce the formation times. The measured formation times are verified by a theoretical estimate based on empirical formulas and by existing breakdown time data in various experimental regimes. The present experimental parameters—significant rise time (~0.5 μs), finite pulse length (~3 μs), and humidity—simulate realistic conditions of high-power millimeter-wave pulses propagating in the atmosphere.

The experimental setup is illustrated in Figure 1. A linearly polarized Gaussian microwave beam is generated by a 1.5 MW, 110 GHz gyrotron oscillator.[20] The beam is focused to a small spot ($1/e$ spot radius w_0 ~4 mm) inside a vacuum chamber by a high-density polyethylene lens, reaching a high enough intensity to cause breakdown in air at atmospheric pressure (peak intensity ~5 MW/cm^2). Breakdown is achieved in a free volume of ambient (laboratory) air, without field-enhancing objects or surfaces nearby. The air pressure in the chamber is varied, and the incident beam power is set approximately near the threshold value at each pressure. Radiofrequency (rf) diode detectors are used to measure the incident power and to observe power reflected from the breakdown plasma.

When breakdown occurs, optical emission is observed visually, and the discharge plasma reflects a significant amount of power. The time delay between when incident power reaches ~95% of full amplitude and when reflected power is first detected by the diode is taken to be the total breakdown delay time τ, as shown in Fig. 2(a). This method allows delay times to be measured with a precision of $\lesssim 0.1$ μs. The rise time of the microwave pulse is 0.5 μs and is very consistent between shots. The total delay time,

$$\tau = \tau_s + \tau_f, \tag{1}$$

is a sum of two components.[2] The statistical delay τ_s represents the waiting time for a seed electron to appear to initiate a breakdown. The formation time τ_f is the exponentiation time of electron avalanche ionization that proceeds from an initial seed electron.

[a]Electronic mail: alancook@mit.edu.

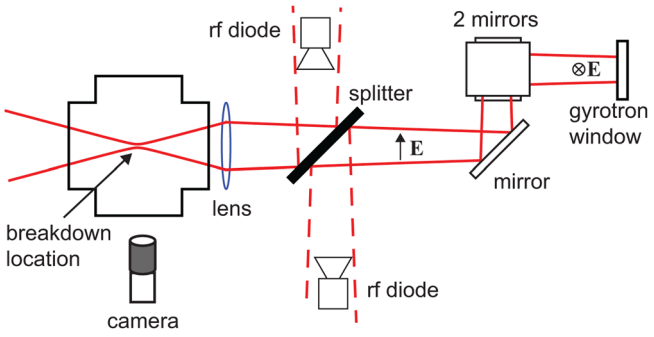

FIG. 1. (Color online) Experimental setup for breakdown delay time measurements.

We use basic breakdown theory to estimate the formation time of air discharges in our experiment. The exponential growth of the free electron density n with time t in a neutral gas subject to an external microwave field is described by

$$n(t) = n_0 e^{(\nu - D/\Lambda^2)t}, \tag{2}$$

a solution to an electron continuity equation, where n_0 is the initial electron density, D is the diffusion coefficient, and $\Lambda = w_0/\pi \approx 1.25$ mm is a characteristic diffusion length[21] quantifying the size of the breakdown region. $\nu = \nu_i - \nu_a$ is the rate at which a free electron produces secondary electrons in ionizing collisions with neutral gas atoms (ν_i, ionizations per electron per second), less the rate at which the electron is lost by attachment to neutral atoms (ν_a). Equation 2 assumes that the external field is uniform in the breakdown region, as are ν and D. This simplifying assumption is useful for estimating basic observable quantities even in non-uniform gas discharge conditions such as this experiment.

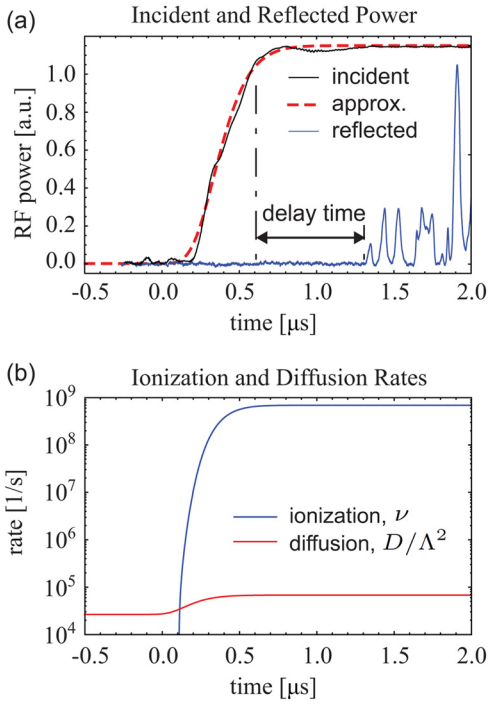

FIG. 2. (Color online) (a) Measured incident power waveform (solid black line) with analytical approximation (dashed red) and normalized reflected power (solid blue). (b) Ionization and diffusion loss rates at 700 Torr during the rise of the microwave pulse, calculated with empirical expressions and $E_{rms}(t)$.

The effective electric field $E_e(t)$ quantifies the efficiency of energy transfer from a microwave field with angular frequency ω to a free electron,[21] and is given by

$$E_e(t) = \frac{E_{rms}(t)}{\sqrt{1 + \omega^2/\nu_c^2}}, \tag{3}$$

where $\nu_c = 5.3 \times 10^9\ p(\text{Torr})\ [\text{s}^{-1}]$ is the rate of collision between an electron and neutral atoms in air as a function of pressure p. The time variation of the root-mean-square field amplitude $E_{rms}(t)$ is calculated using an analytical approximation to the incident microwave pulse shape, which is shown in Fig. 2(a).

The ionization and diffusion rates in air as functions of p(Torr) and $E_e(t)$ (V/cm) are given by empirical formulas, which are valid in the pressure range studied:[21,22]

$$\frac{\nu(t)}{p} = 4 \times 10^7 [(E_e(t)/p)/100]^{5.33} - 6.4 \times 10^4, \tag{4}$$

$$D(t)p = [29 + 0.9(E_e(t)/p)]10^4. \tag{5}$$

Figure 2(b) shows $\nu(t)$ and $D(t)/\Lambda^2$ during the microwave pulse, calculated using Eqs. (3)–(5) for the specific case of $p = 700$ Torr with the incident power near breakdown threshold level.

We apply the analysis used by Foster *et al.*[6] (citing Wijsman[23]) to calculate the probability of a breakdown event forming from a single electron in an ionization avalanche described by Eq. (2). We include electron loss due to diffusion away from the breakdown region, in order to describe our experimental data at low pressure. The probability of an avalanche reaching a size N electrons follow an exponential distribution, given by

$$P(N) = \frac{1}{\bar{n}} e^{-N/\bar{n}}. \tag{6}$$

$\bar{n}$ is the expectation value of N and is equal to Eq. (2) with $n_0 = 1$. For pulsed breakdown conditions where ν and D vary with time, the expectation value at time t into the pulse (starting at $t = 0$) is given by

$$\bar{n}(t) = \exp\left[\int_0^t \{\nu(t') - D(t')/\Lambda^2\} dt'\right]. \tag{7}$$

Breakdown is usually defined as the point where the electron density reaches a critical value n_{cr}. For this analysis, we use $n_{cr} \approx 10^{14}\ \text{cm}^{-3}$, the density at which the plasma frequency is approximately equal to the 110 GHz microwave angular frequency. At this high density, the plasma begins to strongly reflect power. The cumulative probability distribution of breakdown, which is the probability that an avalanche has not reached n_{cr} by time t, is found by integrating Eq. (6) up to n_{cr},

$$P(N < n_{cr}, t) = \int_0^{n_{cr}} P(n) dn. \tag{8}$$

Because we assume the presence of a single electron at $t = 0$, Eq. (8) describes a process governed only by the avalanche amplification statistics, and not by the sources of initial

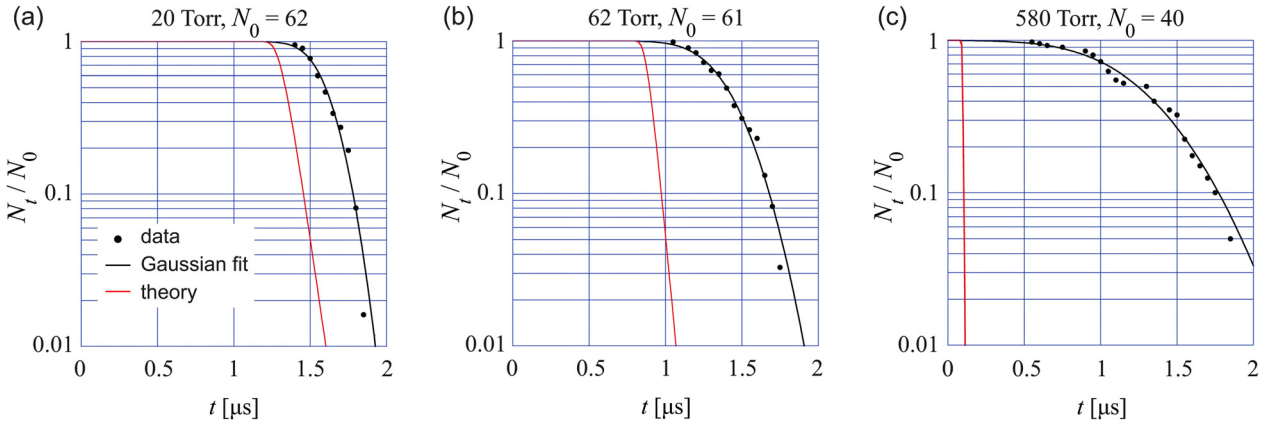

FIG. 3. (Color online) Number of events N_t observed after time t (black circles), as a fraction of total measurement number N_0, at (a) 20 Torr, (b) 62 Torr, and (c) 580 Torr. The solid black curves are Gaussian probability distribution fits to the data. The solid red curves are the theoretical formative distribution of Eq. (8).

seed electrons. The presence of multiple initial electrons would have a negligible effect on the avalanche formation time, as any naturally occurring free electron density is certainly many orders of magnitude below the critical plasma density.

Repeated measurements of the total delay time τ at a fixed pressure and incident power level are shown on a Laue plot,[24] which displays the number of events N_t out of N_0 total measurements that have a delay time greater than t. The Laue plot represents the measured cumulative probability distribution $P(N < n_{cr},t)$. Examples of Laue plots at various pressures for the present 110 GHz breakdown experiment are shown in Fig. 3; 30–60 measurements are taken at each pressure, covering the range 5–700 Torr. The data fits well to the cumulative distribution function for a normal (Gaussian) probability distribution.

The plots in Fig. 3 include the purely formative delay distributions (red curves), calculated with Eq. (8) using Eqs. (3)−(5) as input; the field amplitude E_{rms} used in this calculation was measured at each pressure.[15] The calculated formative distribution is narrow, having a 90%−10% width of 0.1 μs at low pressure and becoming significantly narrower as pressure increases. The wide distribution of measured times is due to statistical delay.[5] We determine the measured formation time at each pressure from the experimental data by the time value on the Gaussian fit curve corresponding to $N_t/N_0 \approx 0.99$, which is essentially the shortest delay time observed.[25]

The maximum statistical delay that we can observe is limited by the microwave pulse length (3 μs). This limit is manifested in the Fig. 3 data as the steadily increasing distribution width as pressure increases; because the formation time at low pressure is close to the length of the microwave pulse, the spread of times that can be observed is narrower. It is clear that there is significant statistical delay ($\gtrsim 1$ μs) near atmospheric pressure (Fig. 3(c)). This indicates an initial absence of naturally occurring free electrons in the breakdown volume. Recent theory and experiments show that detachment of free electrons from negative ion clusters likely plays a large role in providing seed electrons for breakdown in air.[2,4–6]

Figure 4 shows the measured formation times as a function of pressure. The error bars on τ_f are ± 0.1 μs. The data shows reasonable agreement with the Eq. (8) estimate (red line). The observed pressure dependence is due to the relative magnitudes of ν and D/Λ^2 and their different functional dependences on E_e; because ν is a strong function of E_e, the formation time is very sensitive to the incident power level. In the present experiment, the field level was set approximately near the breakdown threshold. The agreement

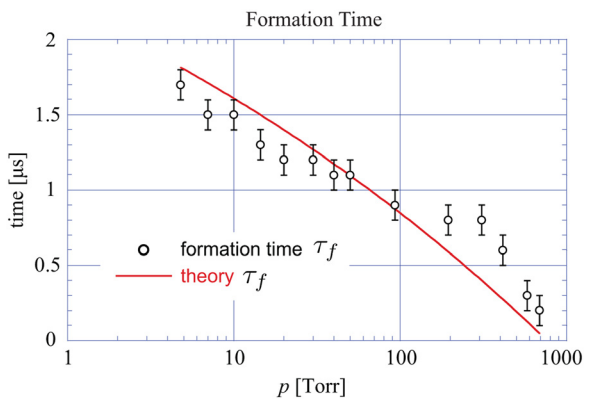

FIG. 4. (Color online) Measured formation time (open circles) versus pressure. The solid red curve is calculated from the formative time distribution theory of Eq. (8)

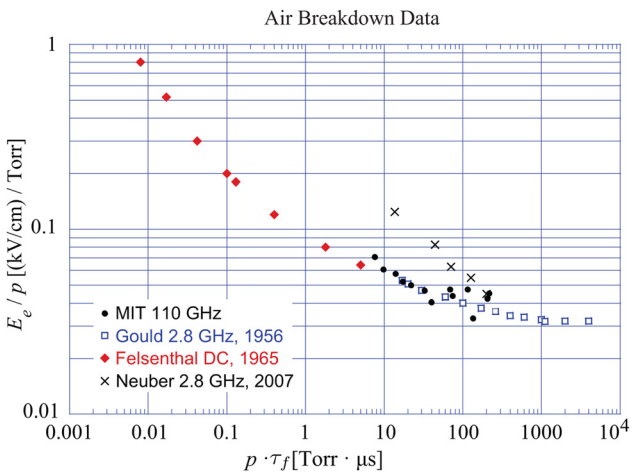

FIG. 5. (Color online) Comparison of breakdown time and field amplitude data between the present 110 GHz experiment (black circles), Gould *et al.*[27] (open squares), Felsenthal *et al.*[28] (red diamonds), and Neuber *et al.*[29] (black crosses).

between the data and the estimate shows that the existing empirical theory is applicable to air discharges in the millimeter-wave regime.

By combining the formation time data with the measured incident field amplitude[15] in a plot of E_e/p vs. $p\tau_f$, we can verify the adherence of 110 GHz pulsed breakdown to the similarity laws of gas discharges. Similarity laws are combinations of physical parameters that can describe the behavior of discharges over a wide range of experimental conditions.[26] Fig. 5 compares data at 110 GHz with the 2.8 GHz data of Gould *et al.*,[27] DC nanosecond pulsed data of Felsenthal *et al.*,[28] and recent 2.8 GHz dielectric surface flashover data of Neuber *et al.*[29] These measurements follow a similar curve, showing that our 110 GHz data is consistent with breakdown time data in other regimes.

This paper presents new data on breakdown plasma formation time in pulsed millimeter-wave air discharges. A beam of 110 GHz radiation is focused to a small spot in a chamber pressurized with ambient (laboratory) air, causing breakdown in a gas volume without surfaces nearby. This allows the discharge formation processes in the gas to be isolated. The observed formation time is in the range $\sim$0.1–2 μs over the pressure range 5–700 Torr, in agreement with a simple pulsed breakdown theoretical estimate. We use gas discharge similarity laws to compare this data with discharge data in other experimental regimes. Near atmospheric pressure we observe an additional statistical time delay of $\gtrsim 1$ μs, which we attribute to the time spent waiting for an initial electron to seed the breakdown avalanche.

This work was supported by AFOSR Grant No. FA9550-09-1-0363 on the Basic Physics of Distributed Plasma Discharges.

[1]R. C. Fletcher, Phys. Rev. **76**, 1501 (1949).
[2]L. G. Christophorou and L. A. Pinnaduwage, IEEE Trans. Electr. Insul. **25**, 55 (1990).
[3]D. Dorozhkina, V. Semenov, T. Olsson, D. Anderson, U. Jordan, J. Puech, L. Lapierre, and M. Lisak, Phys. Plasmas **13**, 013506 (2006).
[4]G. F. Edmiston, A. A. Neuber, H. G. Krompholz, and J. T. Krile, J. Appl. Phys. **103**, 063303 (2008).
[5]J. T. Krile and A. A. Neuber, Appl. Phys. Lett. **98**, 211502 (2011).
[6]J. Foster, H. Krompholz, and A. Neuber, Phys. Plasmas **18**, 013502 (2011).
[7]K. Felch, B. Danly, H. Jory, K. Kreischer, W. Lawson, B. Levush, and R. Temkin, Proc. IEEE **87**, 752 (1999).
[8]K. Sakamoto, A. Kasugai, and K. Takahashi, Nat. Phys. **3**, 411 (2007).
[9]M. K. A. Thumm, Int. J. Infrared Millim. Waves **32**, 241 (2011).
[10]Y. Oda, K. Komurasaki, and K. Takahashi, J. Appl. Phys. **100**, 113307 (2006).
[11]V. Granatstein and G. Nusinovich, J. Appl. Phys. **108**, 063304 (2010).
[12]A. L. Vikharev, A. M. Gorbachev, A. V. Kim, and A. L. Kolysko, Sov. J. Plasma Phys. **18**, 554 (1992).
[13]Y. Hidaka, E. M. Choi, I. Mastovsky, M. A. Shapiro, J. R. Sirigiri, and R. J. Temkin, Phys. Rev. Lett. **100**, 035003 (2008).
[14]Y. Hidaka, E. Choi, I. Mastovsky, M. Shapiro, J. Sirigiri, R. Temkin, G. Edmiston, A. Neuber, and Y. Oda, Phys. Plasmas **16**, 055702 (2009).
[15]A. Cook, M. Shapiro, and R. Temkin, Appl. Phys. Lett. **97**, 011504 (2010).
[16]S. K. Nam and J. P. Verboncoeur, Phys. Rev. Lett. **103**, 055004 (2009).
[17]J.-P. Boeuf, B. Chaudhury, and G. Q. Zhu, Phys. Rev. Lett. **104**, 015002 (2010).
[18]B. Chaudhury, J.-P. Boeuf, and G. Q. Zhu, Phys. Plasmas **17**, 123505 (2010).
[19]Q. Zhou and Z. Dong, Appl. Phys. Lett. **98**, 161504 (2011).
[20]E. Choi, A. Cerfon, I. Mastovsky, M. Shapiro, J. Sirigiri, and R. Temkin, Fusion Sci. Technol. **52**, 334 (2007).
[21]A. D. MacDonald, *Microwave Breakdown in Gases* (Wiley, New York, 1966).
[22]W. C. Taylor, W. E. Scharfman, and T. Morita, *Advances in Microwaves* (Academic, New York, 1971), Vol. 7.
[23]R. A. Wijsman, Phys. Rev. **75**, 833 (1949).
[24]J. M. Meek and J. D. Craggs, *Electrical Breakdown in Gases* (Wiley, New York, 1978).
[25]M. Pejovic, G. Ristic, and J. Karamarkovic, J. Phys. D: Appl. Phys. **35**, R91 (2002).
[26]G. Mesyats, JETP Lett. **83**, 19 (2006).
[27]L. Gould and L. W. Roberts, J. Appl. Phys. **27**, 1162 (1956).
[28]P. Felsenthal and J. Proud, Phys. Rev. **139**, A1796 (1965).
[29]A. A. Neuber, J. T. Krile, G. F. Edmiston, and H. G. Krompholz, Phys. Plasmas **14**, 057102 (2007).